Gene expression patterns in visual cortex during the critical period: Synaptic stabilization and reversal by visual deprivation

Alvin W. Lyckman*†‡, Sam Horng*, Catherine A. Leamey*§, Daniela Tropea*, Akiya Watakabe¶, Audra Van Wart*, Cortina McCurry*, Tetsuo Yamamori¶, and Mriganka Sur*

*Massachusetts Institute of Technology, Picower Institute for Learning and Memory, Cambridge, MA 02139; †Department of Neurology, Tufts University School of Medicine, Caritas St. Elizabeth's Medical Center, Brighton, MA 02135; §Department of Physiology, School of Medical Sciences and Bosch Institute for Medical Research, University of Sydney, Sydney, New South Wales 2006, Australia; and ¶Division of Brain Biology, National Institute for Basic Biology, 38 Nishigonaka Myodaiji, Okazaki 444-8585, Japan

Edited by Joshua R. Sanes, Harvard University, Cambridge, MA, and approved May 1, 2008 (received for review October 25, 2007)

The mapping of eye-specific, geniculocortical inputs to primary visual cortex (V1) is highly sensitive to the balance of correlated activity between the two eyes during a restricted postnatal critical period for ocular dominance plasticity. This critical period is likely to have amplified expression of genes and proteins that mediate synaptic plasticity. DNA microarray analysis of transcription in mouse V1 before, during, and after the critical period identified 31 genes that were up-regulated and 22 that were down-regulated during the critical period. The highest-ranked up-regulated gene, cardiac troponin C, codes for a neuronal calcium-binding protein that regulates actin binding and whose expression is activity-dependent and relatively selective for layer-4 star pyramidal neurons. The highest-ranked down-regulated gene, *synCAM*, also has actin-based function. Actin-binding function, G protein signaling, transcription, and myelination are prominently represented in the critical period transcriptome. Monocular deprivation during the critical period reverses the expression of nearly all critical period genes. The profile of regulated genes suggests that synaptic stability is a principle driver of critical period gene expression and that alteration in visual activity drives homeostatic restoration of stability.

actin | myelin | ocular dominance | synaptic plasticity | troponin

In normal adult mammals, the left and right eyes provide equivalent physiological drive to the binocular parts of visual cortical processing areas. The left-eye versus right-eye responsiveness, or ocular dominance, of cortical neurons can be rapidly and permanently modified by occluding one eye during a brief postnatal developmental period, the critical period for ocular dominance plasticity (1). Brief occlusion of one eye during this critical period leads to an expansion of the cortical representation of the open eye and a regression of that of the closed eye. Ocular dominance plasticity depends on coincidence detection in V1 neurons (2) and involves both long-range geniculocortical inputs and the intrinsic circuitry of V1 (3–5). The robustness, complexity, and experimental accessibility of ocular dominance plasticity give it standing as a platform for gaining molecular insights into mechanisms of cortical adaptation that may operate throughout ontogeny (6).

Several neurobiological processes influence the critical period and/or ocular dominance plasticity *per se*. Early visually driven activity is essential for normal maturation of V1 (7). Ocular dominance plasticity requires development of specific patterns of inhibitory neurotransmission in V1 (8–10). The critical period itself is regulated by the development of inhibitory circuits (11, 12). Elimination of Nogo-R signaling, which involves interactions between neurons and oligodendrocytes, allows for adult plasticity in visual cortex, whereas myelination *per se* appears to be substantially elevated at the close of the critical period (13). Other glial cell functions are also critical: degradation of astrocyte-derived extracellular matrix (14) facilitates ocular dominance plasticity. Neuronal expression of histocompatibility genes is required for normal regulation of ocular dominance plasticity (15). Thus, the critical period for ocular dominance plasticity appears to be defined by the concerted actions of many diverse biological and developmental processes.

It is plausible that the critical period may depend on a particular developmental pattern of transcriptional regulation in V1 that is discernable by unbiased genomic approaches. Previous investigations of molecular regulation of ocular dominance plasticity have largely focused on the effects of activity-dependent processes in V1 (16–21), whereas the question of what intrinsically defines the critical period has received less attention. Here we asked whether a distinct pattern of gene expression exists in V1 during the critical period by analyzing the V1 transcriptome before, during, and after the critical period using DNA microarray analysis. The analysis revealed a distinct transcriptional profile during the critical period that includes unexpected or unknown genes and a relative abundance of genes involving the actin cytoskeleton, G protein signaling, transcription, and myelination. Intriguingly, monocular deprivation (MD) reverses the expression patterns of almost all critical period genes.

Results

Mice of various strains, including C57BL/6, 129S1/Svjae, 129S6/SvEv, and C57/129 hybrids exhibit developmentally regulated ocular dominance plasticity (22–24) [see supporting information (SI) Fig. S1]. Based on the detailed analyses of susceptibility to MD in C57BL/6 mice (22), key parts of which we confirmed in 129S6/SvEv mice (see *Materials and Methods* and *SI Text*), we analyzed the transcriptomes in V1 before the critical period opens [postnatal day 14 (P14)], at the peak sensitivity of the critical period (P28), and after but near the end of the critical period (P60) in 129S6/SvEv mice. To gain additional insight on early developmental regulation, we also examined P0 expression in C57BL/6 mice.

Statistical Analyses of Gene Expression Profiles. Genes were categorized as belonging to one of 24 expression profiles according to their expression levels at the four time points (Fig. S2) and to one of eight patterns of significance (Fig. S3). Two algorithms were used to derive gene expression levels from chip images, MicroArray Suite 5.0 (MAS) (25) and robust multiarray averaging (RMA) (26).

Author contributions: A.W.L., S.H., C.A.L., D.T., A.W., T.Y., and M.S. designed research; A.W.L., S.H., C.A.L., D.T., A.W., A.V.W., and C.M. performed research; A.W.L., S.H., C.A.L., D.T., A.W., A.V.W., C.M., T.Y., and M.S. analyzed data; and A.W.L. and M.S. wrote the paper.

The authors declare no conflict of interest.

This article is a PNAS Direct Submission.

Data deposition: The microarray data reported in this paper have been deposited in the Gene Expression Omnibus (GEO) database, www.ncbi.nlm.nih.gov/geo (accession no. GSE11764).

‡To whom correspondence should be addressed. E-mail: alvin.lyckman@tufts.edu.

This article contains supporting information online at www.pnas.org/cgi/content/full/0710172105/DCSupplemental.

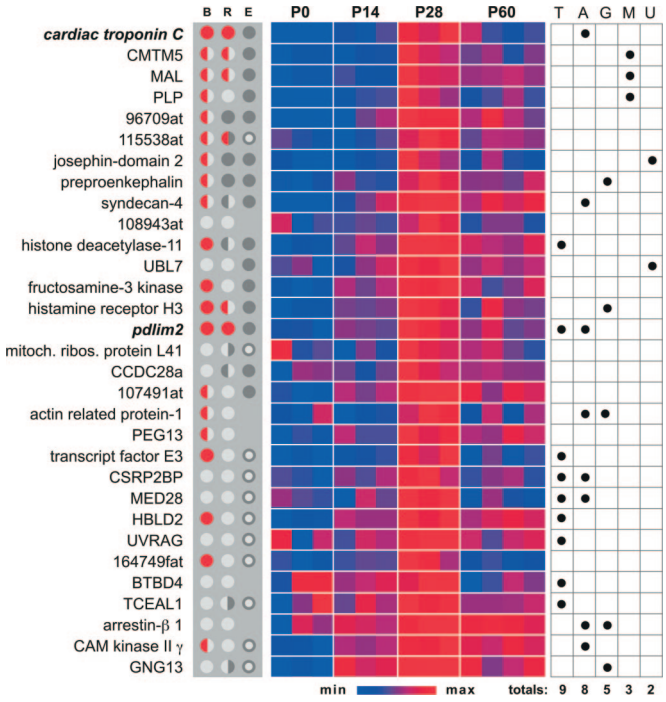

Fig. 1. Genes showing significant peak expression at P28 from the MAS expression data, ranked in descending order by their P28/P14 ratios. Gene names or Affymetrix probe set designations are given to the left. Color maps indicate a gene's relative expression in each sample with red showing the highest and blue showing the lowest. *Cardiac troponin C* had the highest P28/P14 fold change (3.3). Column B, Bonferroni post hoc tests. A filled half circle indicates $P < 0.05$ (left half, P14 v. P28; right half, P28 v. P60). Column R, RMA dataset. A filled half circle indicates $P < 0.05$ for the *t* test (dark) or Bonferroni post hoc test (red) using the corresponding MAS dataset (left and right as for B). Column E, expression profiles. A filled circle indicates identical expression profiles (type 13) for both the MAS and RMA datasets; a hollow circle indicates peak expression at P28 for both MAS and RMA profiles (but not type 13). Functional attributes for each gene are indicated to the right: A, actin cytoskeleton interaction; G, G protein signaling; M, myelination; T, transcription; U, ubiquitin/proteasome. Counts for each category are given underneath.

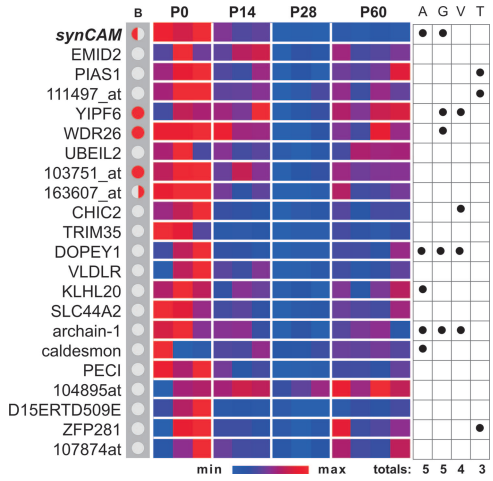

Fig. 2. Genes showing significant minimal expression at P28 from the MAS expression data, ranked in descending order by their P14/P28 ratios. *synCAM* had the highest P14/P28 fold change (4.9). Column B, Bonferroni post hoc tests are as described in Fig. 3. A, actin cytoskeleton interaction; G, G protein signaling; V, vesicular transport; T, transcription.

Although MAS and RMA are computationally distinct, their resulting datasets were strongly correlated ($r^2 = 0.70$, $P < 10^{-20}$). The MAS dataset, which also provides a presence call statistic (27), is relied on for the bulk of this presentation. See Fig. S3, Dataset S1, and Dataset S2 for details of the MAS versus RMA comparisons.

Cross-Validation by Semiquantitative RT-PCR. Microarray data were compared with data from semiquantitative analysis of RT-PCR experiments (Fig. S4). Regardless of the expression profile, the microarray datasets were strongly correlated with the RT-PCR data. These analyses provided cross-validation of the microarray data with an independent biochemical assay of gene expression.

Critical Period Gene Expression: Up-Regulation. We assumed *a priori* that expression profiles with strong functional relevance to critical period plasticity are those with significant extremes of expression during the critical period. Genes were considered up-regulated critical period genes if they had a significant peak in expression at P28 (i.e., $P < 0.05$ for P14 versus P28 and for P28 versus P60), a minimum 1.25-fold increase in expression between P14 and P28, and an average presence call of at least 33% at P28. This analysis identified 31 genes that were up-regulated at P28 in the MAS dataset (Fig. 1). The most common expression profile was type 13, in which expression levels ranked P28 > P60 > P14 > P0 (Fig. S2).

Of these 31 genes, *cardiac troponin C* (*cTropC*) (28, 29) and *pdlim2* (30) also showed significant up-regulation as assessed by ANOVA/B in both the MAS and RMA datasets (Fig. S5). As ordered by the fold increase between P14 and P28, *cTropC* ranked first and *pdlim2* ranked 15th. Of interest is that the two statistically strongest up-regulated genes, *cTropC* and *pdlim2*, both have prominent association with the actin cytoskeleton, a function that accounts for 26% of the 31 up-regulated genes. The second, third, and fourth highest-ranked up-regulated genes, *CKLF-like MARVEL transmembrane domain-containing protein 5* (*CMTM5*), *myelin and lymphocyte protein* (*MAL*), and *proteolipid protein 1* (*PLP1*), respectively, code for proteins involved in myelination. Additional categories of cell biological function that were prominently represented were transcription (29%) and G protein signaling (13%) (Fig. 1).

Analogous statistical analyses applied to the RMA dataset identified 22 up-regulated genes (Fig. S5). Fifteen of these 22 genes had expression profile type 13 in both the MAS and RMA datasets. Three of these up-regulated genes are associated with the actin cytoskeleton: *myosin light chain 4* (ranking first), *cTropC* (fourth), and *pdlim2* (15th). A myelination-related gene, *myelin-associated oligodendrocyte basic protein* (*MOBP*), ranked third. G protein signaling (23%) and actin cytoskeleton (23%) were the most frequently represented functional categories in this list.

Critical Period Gene Expression: Down-Regulation. Critical period plasticity may be facilitated by down-regulation of genes that inhibit synaptic plasticity. We identified 22 genes in the MAS dataset that were significantly down-regulated at P28, with P14 expression levels being at least 1.3-fold greater than P28 levels (Fig. 2). When ranked by their decreasing P14/P28 ratios, the highest-ranked gene was *synCAM* (31), a gene that along with two other down-regulated genes encodes gene products associated with the actin cytoskeleton. *synCAM* expression was elevated 9-fold ($P < 0.009$) in response to MD—the third-highest such response in the entire dataset. *synCAM* and two other down-regulated genes also have G protein signaling function. In the RMA dataset, no genes that were significantly down-regulated at P28 had more than a 20% reduction at P28, and none was given further consideration.

Effects of MD. Examination of the activity dependence of critical period gene expression at P28 was tested by MD (20) and analyzed by MAS and Student's *t* test. Across the entire transcriptome, 53.8%

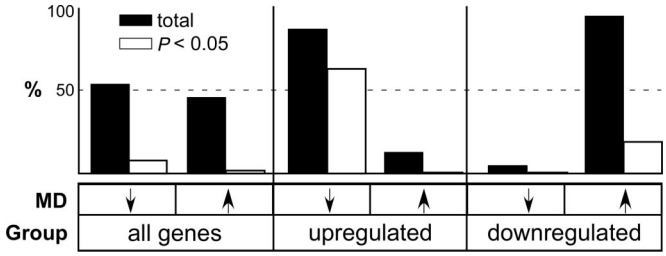

Fig. 3. Selective reversal of critical period gene expression patterns by MD at P28. After MD, average gene expression as measured by microarray analysis was either reduced (downward arrows) or elevated (upward arrows) as compared with non-MD samples. Filled bars show all genes in group. Open bars show significant changes. (*A*) MD changed average gene expression levels by ≈50% for all genes. (*B*) For those genes that were developmentally up-regulated during the critical period, the vast majority had reduced expression in response to MD. (*C*) Conversely, MD elevated the P28 expression levels for almost all genes that were developmentally down-regulated during the critical period.

of genes were reduced by MD (with 7.8% being significant), whereas 46.2% were elevated by MD (with 1.7% being significant) (Fig. 3*A*). It is plausible that MD would increase the expression of genes that mediate critical period plasticity (presumably the up-regulated genes) and conversely decrease the expression of genes that inhibit plasticity (presumably the down-regulated genes). In fact, we found exactly the opposite scenario. The expression of 27 (87%) of the 31 up-regulated genes (Fig. 1) was decreased by MD, an effect that was significant for 17 (63%) genes (Fig. 3*B*). Conversely, for the 22 genes that were down-regulated during the critical period (Fig. 2), 95% had increased expression after MD, of which 19% were significantly increased (Fig. 3*C*). Thus, MD reverses the expression patterns of almost all critical period genes.

Biological and Developmental Processes Associated with Ocular Dominance Plasticity. Microarray analysis provides the opportunity to determine whether particular functional categories of genes are associated with critical period plasticity. Here, four such categories are considered for genes with significant expression profiles: process outgrowth, synaptogenesis, inhibitory neurotransmission, and myelination. Ocular dominance plasticity involves extensive synaptic rearrangement, which is plausibly facilitated by elevated expression of molecules required for process outgrowth and the formation of synaptic connections. Although these two categories have many proteins in common, the "process outgrowth" category (Fig. 4*A*) tends to have proteins most strongly associated with axonal and dendritic neuritogenesis, whereas the "synaptogenesis" category (Fig. 4*B*) contains canonical proteins of the synapse and synaptic transmission. These two categories showed different expression profiles. Process outgrowth genes tended to peak at P0 and sharply decline by P14. One of these genes, *protocadherin-9*, showed a significant 4-fold elevation in expression in response to MD at P28 (Fig. 4*A*). The synaptogenesis category (Fig. 4*B*) showed a dramatic up-regulation from P0 to P14 and a gradual decline through P60. This pattern of expression is consistent with intense synaptogenesis between P0 and P14 (32). Taken together, these data do not support the hypothesis that the critical period stems from a resurgence of expression of genes that mediate process outgrowth or synaptogenesis, although the elevated expression of synaptogenesis genes may facilitate ocular dominance plasticity. Finally, the patterns of expression for the process outgrowth and the synaptogenesis genes are highly consistent with numerous reports of their developmental regulation, and thus these analyses also provide extensive corroboration of the microarray data.

Expression Patterns of Genes Associated with Inhibitory Neurotransmission. Considerable experimental evidence indicates that ocular dominance plasticity is critically dependent on the normal maturation of inhibitory synaptic connections in V1. Expression profiles of genes associated with inhibition (Fig. 4*C*) are in general similar to those for genes associated with synaptogenesis (Fig. 4*B*). *BDNF* expression, essential for normal development of cortical GABAergic neurons, is lowest at P0 and rises to an expression plateau by P28. In addition, four GABA-A receptor subunits had significantly elevated expression in response to MD (Fig. 4*C*). These data indicate that many genes associated with inhibitory circuitry are intensely expressed before, and throughout, the critical period.

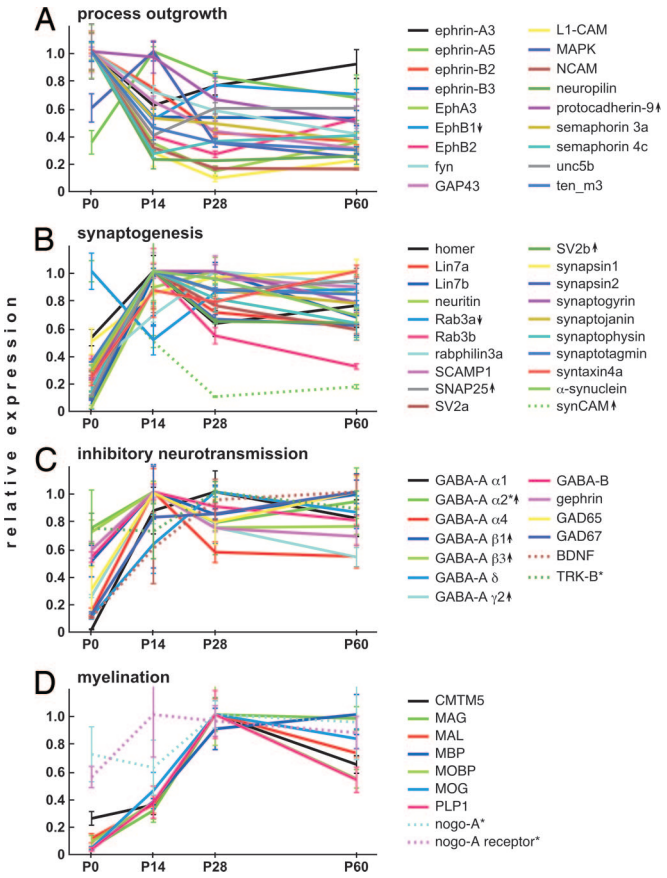

Fig. 4. Developmental regulation of genes involved in process outgrowth (*A*), synaptogenesis (*B*), inhibitory neurotransmission (*C*), and myelination (*D*). In general, gene expression peaked at P0 for process outgrowth, at P14 for synaptogenesis and inhibitory neurotransmission, and at P28 for myelination. *BDNF* (required for the development of inhibitory circuits) steadily increased its expression between P0 and P60, but its receptor's (*trkB*) expression profile was not significant (dashed lines in *C*). Neither *nogo-A* nor its receptor (*nogo-A receptor*) was significant (dashed lines in *D*). Data are average MAS expression level ± SEM. *, no significant changes in expression but included because of functional relevance. Arrows indicate significant elevation (up) or reduction (down) in response to MD. Note that P0 expression data were obtained from C57BL/6 mice, whereas the P14, P28, and P60 data were from 129S6/SvEv mice.

Expression Patterns of Myelination Genes. Recent findings that myelination and *nogo* signaling may inhibit ocular dominance plasticity (13) suggested that the expression of genes associated with myelination might be reduced during the critical period. However, four myelination genes were significantly up-regulated at the peak of the critical period (Fig. 2 and Fig. S5). To further assess whether myelination is correlated with the critical period, expression patterns of nine canonical oligodendrocyte and myelination-related genes, including the genes encoding *nogo-A* (*reticulon-4A*, expressed by oligodendrocytes and neurons) and the *nogo-A receptor* (*reticulon-4A receptor*, expressed predominantly by neurons), were examined collectively (Fig. 4*D*). The myelination-associated genes

NEUROSCIENCE

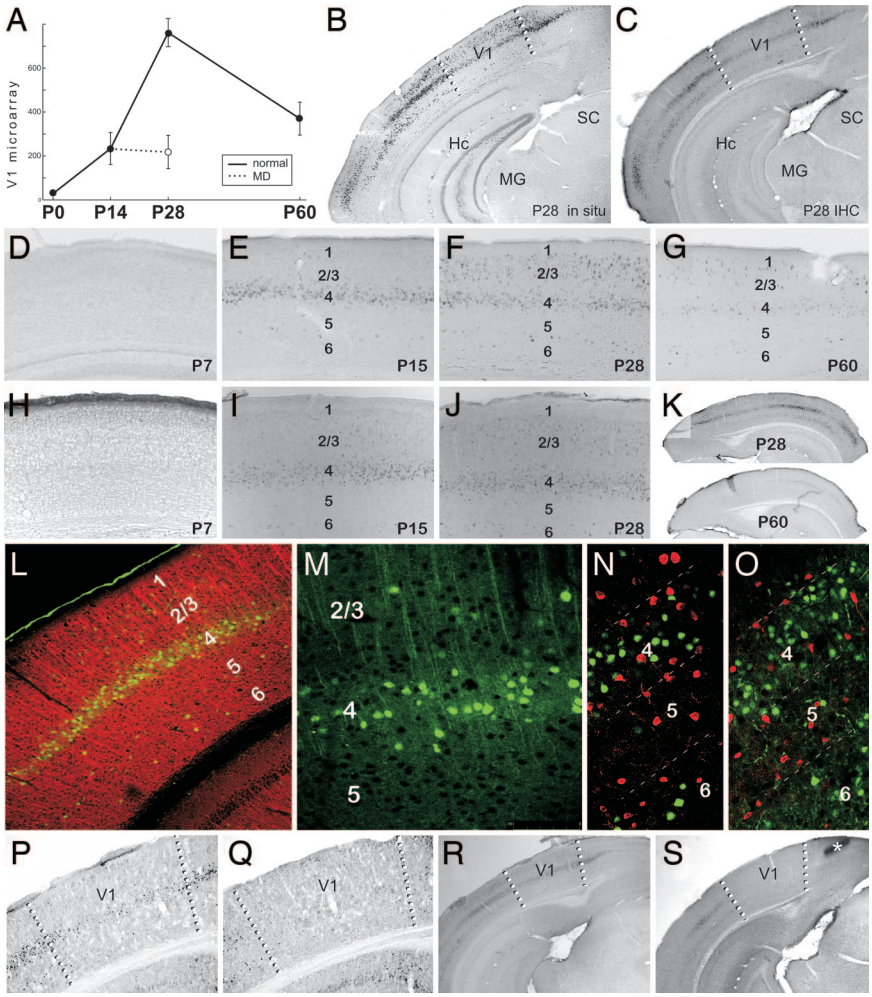

Fig. 5. Cardiac troponin C (cTropC) expression occurs predominantly in layer-4 excitatory neocortical neurons and is regulated by development and visual activity. (*A*) cTropC expression peaked at P28 (solid line); MD significantly reduced its expression at P28 (dashed line). Data show MAS expression values ± SEM. (*B* and *C*) P28 coronal sections showing V1 stained for cTropC mRNA by *in situ* hybridization (*B*) and cTropC protein by immunohistochemistry (*C*). SC, superior colliculus; MG, medial geniculate nucleus; Hc, hippocampus. Staining predominates in layer 4 of the neocortex, although stretches of staining occur in the upper part of layers 2/3 and in layer 6 in several neocortical regions. (*D–J*) Coronal sections of the extent of V1 (pia up, dorsomedial edge to the left) at P7, P15, P28, and P60. (*K*) Coronal sections (dorsal left, medial down) at P28 and P60 of posterior cortex. *In situ* hybridizations (*D–G*) and immunohistochemical staining (*H–K*) are shown. Layer 4 is intense by P15 (*E* and *I*). Layers 2/3 and 6 are stronger by P28 (*F* and *J*). Expression waned by P60 (*G* and *K*). (*L*) Confocal image of double immunofluorescence staining of cortical neurons for cTropC (green) and the neuronal marker MAP2 (red). (*M*) At higher power, cTropC staining was nuclear, perinuclear, and dendritic. (*N* and *O*) cTropC immunoreactivity (green) shows no colocalization with either GABA (*N*, red) or parvalbumin (*O*, red). (*P* and *Q*) Brief (2-day, P26–P28) MD substantially eliminated cTropC expression in the V1 contralateral (*Q*) versus ipsilateral (*P*) to the closed eye. (See Fig. S6 for a broader view of the cortex.) (*R* and *S*) Brief (2-day, P26–P28) dark rearing substantially eliminated cTropC-positive neurons in V1 (*S*) as compared with that in an untreated P28 littermate (*R*). The asterisk in *S* indicates a tear in the section that caused a staining artifact. Strains used: 129S6/SvEv in *C*, *H–O*, *R*, and *S*; C57BL/6 in *B*, *D–G*, *P*, and *Q*.

showed significant up-regulation at P28, whereas *nogo-A* and *nogo-A receptor* showed no significant changes in expression profile (Fig. 4*D*). In response to MD, expression was elevated for four of these genes and reduced for the other five, but none of these changes was significant (Fig. 4*D*). Myelination, therefore, appears to be delayed with respect to synaptogenesis and the development of inhibitory circuitry yet vigorous during the critical period.

Novel Ocular Dominance Plasticity Candidate: Cardiac Troponin C (cTropC). A major strength of unbiased bioinformatics is the potential to identify genes not previously associated with a specific biological function. Such is the case for cTropC (Fig. 5), a protein known to regulate the Ca^{2+}-dependent interaction between actin filaments and the myosin-ATPase in muscle fibers. *cTropC* is highly up-regulated during the critical period (Figs. 1 and 5 and Figs. S4 and S5), and its expression is significantly ($P < 0.0001$) reduced in response to MD (Fig. 5*A*). *In situ* hybridization to the *cTropC* transcript (Fig. 5*B*) or immunohistochemical staining for cTropC protein (Fig. 5*C*) revealed striking laminar and region-specific expression patterns in the neocortex. cTropC expression was strongly elevated across the neocortex in layer 4 (Fig. 5 *C* and *D*), a layer with few known selective markers (33). There was also significant expression in layers 2/3 and layer 6 in several neocortical areas.

Although the histological staining methodologies are not strictly quantitative, the labeling intensity was consistent with relatively strong critical period expression of *cTropC* mRNA (Fig. 5 *D–G*) and protein (Fig. 5 *H–K*) in V1. Layer-4 staining appeared strong at both P15 and P28. The significantly elevated cTropC expression at P28 versus P14 in the microarray data (Fig. 5*A*) may be reflected by the apparent onset of cTropC expression in layers 2/3 and 6 at P28 (Fig. 5 *D* and *E*). Sections from P28 and P60 mice when reacted together in the same immunohistochemical staining reactions indicate a steep drop in immunoreactivity between P28 and P60 (Fig. 5*K*). Strong, cortical neuron-specific cTropC staining is evident outside V1 (Fig. 5 *B*, *C*, and *G*). No labeling was detected at P7 by either *in situ* hybridization (Fig. 5*D*) or immunohistochemistry (Fig. 5*H*).

At the cellular level, cTropC protein expression was restricted to neurons (MAP2-positive cells) (Fig. 5*L*). The subcellular localization (Fig. 5*M*) would be consistent with a dendritic nuclear Ca^{2+}-signaling function, although this is speculative at present. Cellular morphologies of cTropC-positive neurons in layer 4 were consistent with those of the excitatory star pyramidal neuron class that receives thalamic inputs (34). In agreement with this hypothesis, cTropC-positive neurons did not overlap with inhibitory GABAergic neurons (Fig. 5*N*) or parvalbumin-positive neurons (Fig. 5*O*). Finally, brief (2-day) loss of monocular (Fig. 5 *P* and *Q*) or binocular (Fig. 5 *R* and *S*) visual activity during the critical period substantially eliminated cTropC immunoreactivity in V1 neurons.

Discussion

The present study has examined changes in the transcriptome in V1 before, during, and after the juvenile critical period in mice to identify developmentally regulated genes that encode proteins involved in ocular dominance plasticity. This study has generated a

set of unexpected findings and some previously undescribed conclusions. First, candidate molecular components of ocular dominance plasticity have been identified. Second, the findings permit an overview of the molecular mechanisms that regulate synaptic plasticity during the critical period and reveal an antagonistic interaction between development driven by normal binocular vision and that due to unbalanced drive between the two eyes. It is important to note that recent evidence indicates that adult visual cortex is capable of expressing ocular dominance plasticity (35) and homeostatic plasticity (36) and that these forms of plasticity in the adult appear to be mechanistically distinct from that which occurs in the juvenile critical period.

The present study documents the unexpected finding of significant expression of a novel neuronal protein, cardiac troponin C. In heart and skeletal muscle, troponin C is the Ca^{2+}-binding element of the tripartite troponin complex that regulates the Ca^{2+}-dependent interaction between actin and myosin through allosteric interactions with tropomyosin. Expression of cardiac troponin C or other troponin isoforms in cerebral cortex has received scant attention (28, 37). Its expression peaks strongly in V1 in the critical period. It also shows highly prominent localization to the cell bodies and dendrites of layer-4 excitatory neurons, as well as expression in neurons in layers 2/3 and 6. These findings, together with its known functional properties, suggest a link between Ca^{2+} regulation and actin binding in ocular dominance plasticity during the critical period. As a technical note, caution may be warranted in the application of cardiac troponin C as a Ca^{2+} indicator (38, 39) because it may interfere with normal Ca^{2+}-dependent signaling in cortical neurons under certain conditions.

Two other highly significant candidate genes not previously associated with ocular dominance plasticity have been identified. *Pdlim2*, another significantly up-regulated candidate gene, encodes isoforms that interact with the actin cytoskeleton and that translocate to the nucleus (30). *Pdlim2* expression was significantly reduced in response to MD. The most prominent down-regulated gene, *synCAM*, encodes a protein component of synaptic cell–cell adhesion complexes with actin binding domains. *synCAM* expression was intensely up-regulated by MD.

Functional candidate molecules are frequently identified first by patterns of expression that put the molecules at the right place and at the right time to contribute to a biological process. However, with regard to ocular dominance plasticity, the present study is somewhat counterintuitively conformant with this principle. What is interesting about most of the genes that are up-regulated (or down-regulated) during the critical period is that the stimulus that elicits ocular dominance plasticity reduces (or elevates) their expression. Negative feedback or homeostatic mechanisms that are driven by changes in correlated or total activity (40) might explain some of these responses. Equally importantly, however, this finding suggests that the critical period for ocular dominance plasticity can also be readily understood as a period of amplified synaptic stability; i.e., the expression patterns of critical period genes can be parsimoniously explained if they serve to consolidate extant connections in lieu of adding new ones, so long as the balance of correlated activity is maintained. This may be appropriate given that the critical period follows an epoch of intense perinatal synaptogenesis (32). Such consolidation is consistent with the increased frequency of spontaneous transmission observed in the developing visual cortex (41). Thus, in the case of *synCAM*, which encodes a cell–cell adhesion protein required for synaptogenesis and maturation of presynaptic terminals (31, 42), its expression is down-regulated during the critical period (maintaining synaptic stability) but is strongly up-regulated in response to MD (fostering formation of new synaptic connections). SynCAM therefore fits the model of a protein necessary for ocular dominance plasticity, which is normally down-regulated during the critical period. Although binocular competition has largely driven thinking about ocular dominance plasticity, recent data show that homeostatic plasticity of cortical connections is robustly expressed in monocularly driven neurons in response to MD (41, 43, 44), and such plasticity may be related to the homeostasis of gene regulation described here.

Conversely, *cardiac troponin C*, a strongly up-regulated gene, is likely to contribute to synaptic stability during the critical period. Cardiac troponin C is an avid calcium binding protein, and this activity would permit it to function either as a Ca^{2+} buffer or as a transducer in a Ca^{2+}-signaling cascade, particularly in the input layer of V1. However, because its expression is rapidly reduced in response to brief visual deprivation, it is plausible that it normally inhibits Ca^{2+} signaling that is required for ocular dominance plasticity. During visual deprivation, this inhibition would be relieved, and signaling that is permissive for synaptic rearrangements would proceed unimpeded. Thus, it is convenient to posit that the critical period function of cardiac troponin C, as well as the many other up-regulated critical period genes, is to promote synaptic stability. How activity might regulate these gene expression responses is perhaps more elusive, because it is arguable that such a detection system *per se* should be immune from development- and activity-driven modulation in expression level. However, the regulated transcriptional elements detected in the present study may be components of this system.

Regulation of the actin cytoskeleton and myelination are salient features of critical period gene regulation. The actin cytoskeleton has critical function in the stabilization and trafficking of receptors and channels (45) and, as a major structural component of growth cones (46) and dendritic spines (47), in the dynamics of process outgrowth. Developmental down-regulation of dendritic spine motility during the critical period, and its elevation by visual deprivation, may be related to the function of this category of genes (32, 48). Another prominent category of cellular function that contributes to critical period gene expression, G protein signaling, is tightly coupled to the regulation of the synaptic actin cytoskeleton (49). Gene activity consistent with strong myelinating activity occurs during the critical period, whether or not visual deprivation occurs. As a cautionary note, it is important to note that the present study has not addressed the extent to which up-regulation of myelination genes led to an increase in myelin production. Application of differential proteomics techniques may facilitate answering such questions (21). Nonetheless, the present findings need to be reconciled with the hypothesis that myelination impedes ocular dominance plasticity (13). Myelination may signal the closing of plasticity windows (50), but in other neural systems functional plasticity appears to be supported by ongoing myelinating activity (51).

In summary, the large range of genes that are up- or down-regulated during the critical period and the multiple categories to which they belong underscore the diversity and complexity of processes that must be coordinated to establish and consolidate synapses in visual cortex during development. The genes we have discovered, dominated by genes associated with the actin cytoskeleton, G protein signaling, transcription, and myelination, significantly extend the known molecular pathways associated with synaptic development and plasticity in visual cortex during the critical period. The unexpected antagonism between unbalanced binocular drive and normal development suggests that homeostatic regulatory forces generate a functional dichotomy within the critical period: an enhanced capacity for synaptic plasticity after unbalanced visual activity that coexists with a default propensity for synaptic stabilization under normal conditions.

Materials and Methods

Animals and Experimental Design. This study was conducted with mouse strains 129S6/SvEv and C57BL/6 (Taconic). All procedures on live animals were approved by the Institutional Animal Care and Use Committees at Massachusetts Institute of Technology and Caritas St. Elizabeth's Medical Center. Mouse colonies were maintained under standard conditions of 12-h on/12-h off light cycle, with access to water and chow ad libitum (Guide for the Care and Use of Laboratory Animals, National Research Council). No additional visual enrichment was provided. Litters

of 8–12 129S6/SvEv mice from three age groups were used to analyze changes in the transcriptome from V1 (including the monocular region, binocular region, and all layers) before (P14, $n = 3$ litters), during (P28, $n = 3$ litters), and after (P60, $n = 4$ litters) the critical period for ocular dominance plasticity. To better understand the early postnatal regulation of these genes, we also analyzed the transcriptome in V1 in three litters of C57BL/6 mice at P0. Analysis of gene expression changes in MD experiments was done on three litters of 129S6/SvEv mice. Each litter in each age or treatment group ($n = 16$) was processed in a separate, independent experiment. The Affymetrix MG-U74v2 microarray set was used to measure the transcriptome of V1. Details of the tissue dissection and processing, cRNA preparation, and hybridization are provided in *SI Text*. Raw microarray images were processed with Microarray Suite 5 (MAS) (25) or the RMA protocol (26) to obtain normalized expression level measurements. Refer to *SI Text* for details. A subset of genes of potential functional significance representing various developmental expression patterns was to verify the expression data using semiquantitative RT-PCR. Refer to *SI Text* for details.

In Situ Hybridization. A near full-length, digoxigenin-labeled RNA probe for cardiac troponin C (cTropC, National Center for Biotechnology Information accession no. M29793, probe target = 85–603, CDS = 44–529) was hybridized to floating sections of mouse brain and revealed by using an anti-digoxigenin primary antibody and an alkaline phosphatase-coupled secondary antibody using C57BL/6 mice as described (33).

Immunolocalization. A monoclonal antibody (USBiological) against cTropC (1:250) was used to stain mouse brain sections from 129S6/SvEv mice by peroxidase-based immunohistochemistry and double immunofluorescence staining. Double immunofluorescence staining was done with antibodies to MAP2 (Sigma; 1:1,000), parvalbumin (Chemicon; 1:1,000), and GABA (Sigma; 1:1,000) using Alexa Fluor secondary antibodies (Invitrogen; 1:400). Brightfield digital images were captured on a Zeiss Axiophot system, and fluorescence was captured on a Zeiss 510 Meta laser-scanning confocal system.

Visual Deprivation. Ocular dominance plasticity was confirmed in 129S6/SvEv mice by using optical imaging (see Fig. S1 for details). Changes in gene expression in response to MD in 129S6/SvEv mice (20) were determined by statistical comparison with the untreated P28 mice using MAS. Acute effects on cardiac troponin C expression were examined by treating C57BL/6 mice for 2 days with either MD or dark rearing, and analyzed by immunohistochemistry as described (48).

ACKNOWLEDGMENTS. We thank Charlene Ellsworth, Serkan Oray, and James Schummers (MIT); Matthew Perkins and Gloria Fang (CSEMC); and Sonoko Ohsawa (NIBB) for technical assistance. Dr. Kenneth Rosen provided a critical reading of the manuscript. This work was supported by research grants from the National Institutes of Health and the Simons Foundation (to M.S.) and institutional funding from Caritas St. Elizabeth's Medical Center (to A.W.L.).

1. Hubel DH, Wiesel TN (1970) The period of susceptibility to the physiological effects of unilateral eye closure in kittens. *J Physiol* 206:419–436.
2. Kleinschmidt A, Bear MF, Singer W (1987) Blockade of ''NMDA'' receptors disrupts experience-dependent plasticity of kitten striate cortex. *Science* 238:355–358.
3. Trachtenberg JT, Trepel C, Stryker MP (2000) Rapid extragranular plasticity in the absence of thalamocortical plasticity in the developing primary visual cortex. *Science* 287:2029–2032.
4. Antonini A, Fagiolini M, Stryker MP (1999) Anatomical correlates of functional plasticity in mouse visual cortex. *J Neurosci* 19:4388–4406.
5. Shatz CJ, Stryker MP (1978) Ocular dominance in layer IV of the cat's visual cortex and the effects of monocular deprivation. *J Physiol* 281:267–283.
6. Pascual-Leone A, Amedi A, Fregni F, Merabet LB (2005) The plastic human brain cortex. *Annu Rev Neurosci* 28:377–401.
7. Mower GD, Berry D, Burchfiel JL, Duffy FH (1981) Comparison of the effects of dark rearing and binocular suture on development and plasticity of cat visual cortex. *Brain Res* 220:255–267.
8. Hensch TK, *et al.* (1998) Local GABA circuit control of experience-dependent plasticity in developing visual cortex. *Science* 282:1504–1508.
9. Iwai Y, Fagiolini M, Obata K, Hensch TK (2003) Rapid critical period induction by tonic inhibition in visual cortex. *J Neurosci* 23:6695–6702.
10. Huang ZJ, *et al.* (1999) BDNF regulates the maturation of inhibition and the critical period of plasticity in mouse visual cortex. *Cell* 98:739–755.
11. Hanover JL, Huang ZJ, Tonegawa S, Stryker MP (1999) Brain-derived neurotrophic factor overexpression induces precocious critical period in mouse visual cortex. *J Neurosci* 19:RC40.
12. Gianfranceschi L, *et al.* (2003) Visual cortex is rescued from the effects of dark rearing by overexpression of BDNF. *Proc Natl Acad Sci USA* 100:12486–12491.
13. McGee AW, Yang Y, Fischer QS, Daw NW, Strittmatter SM (2005) Experience-driven plasticity of visual cortex limited by myelin and Nogo receptor. *Science* 309:2222–2226.
14. Pizzorusso T, *et al.* (2002) Reactivation of ocular dominance plasticity in the adult visual cortex. *Science* 298:1248–1251.
15. Syken J, Grandpre T, Kanold PO, Shatz CJ (2006) PirB restricts ocular-dominance plasticity in visual cortex. *Science* 313:1795–1800.
16. Lachance PE, Chaudhuri A (2004) Microarray analysis of developmental plasticity in monkey primary visual cortex. *J Neurochem* 88:1455–1469.
17. Majdan M, Shatz CJ (2006) Effects of visual experience on activity-dependent gene regulation in cortex. *Nat Neurosci* 9:650–659.
18. Ossipow V, Pellissier F, Schaad O, Ballivet M (2004) Gene expression analysis of the critical period in the visual cortex. *Mol Cell Neurosci* 27:70–83.
19. Prasad SS, *et al.* (2002) Gene expression patterns during enhanced periods of visual cortex plasticity. *Neuroscience* 111:35–45.
20. Tropea D, *et al.* (2006) Gene expression changes and molecular pathways mediating activity-dependent plasticity in visual cortex. *Nat Neurosci* 9:660–668.
21. Van den Bergh G, Clerens S, Firestein BL, Burnat K, Arckens L (2006) Development and plasticity-related changes in protein expression patterns in cat visual cortex: A fluorescent two-dimensional difference gel electrophoresis approach. *Proteomics* 6:3821–3832.
22. Gordon JA, Stryker MP (1996) Experience-dependent plasticity of binocular responses in the primary visual cortex of the mouse. *J Neurosci* 16:3274–3286.
23. Muhammad R, Heynen AJ, Bear MF, Sheng M (2007) Strain differences in visual function and ocular dominance plasticity revealed using visually evoked potentials in the awake mouse. *Soc Neurosci Abstr* 32:130.9.
24. Taha SA, Stryker MP (2005) Ocular dominance plasticity is stably maintained in the absence of alpha calcium calmodulin kinase II (alphaCaMKII) autophosphorylation. *Proc Natl Acad Sci USA* 102:16438–16442.
25. Hubbell E, Liu WM, Mei R (2002) Robust estimators for expression analysis. *Bioinformatics* 18:1585–1592.
26. Irizarry RA, *et al.* (2003) Exploration, normalization, and summaries of high density oligonucleotide array probe level data. *Biostatistics* 4:249–264.
27. Choe SE, Boutros M, Michelson AM, Church GM, Halfon MS (2005) Preferred analysis methods for Affymetrix GeneChips revealed by a wholly defined control dataset. *Genome Biol* 6:R16.
28. Berezowsky C, Bag J (1992) Slow troponin C is present in both muscle and nonmuscle cells. *Biochem Cell Biol* 70:691–697.
29. Parmacek MS, Leiden JM (1989) Structure and expression of the murine slow/cardiac troponin C gene. *J Biol Chem* 264:13217–13225.
30. Loughran G, *et al.* (2005) Mystique is a new insulin-like growth factor-I-regulated PDZ-LIM domain protein that promotes cell attachment and migration and suppresses anchorage-independent growth. *Mol Biol Cell* 16:1811–1822.
31. Biederer T, *et al.* (2002) SynCAM, a synaptic adhesion molecule that drives synapse assembly. *Science* 297:1525–1531.
32. Konur S, Yuste R (2004) Developmental regulation of spine and filopodial motility in primary visual cortex: Reduced effects of activity and sensory deprivation. *J Neurobiol* 59:236–246.
33. Watakabe A, *et al.* (2007) Comparative analysis of layer-specific genes in mammalian neocortex. *Cereb Cortex* 17:1918–1933.
34. Peters A, Kara DA (1985) The neuronal composition of area 17 of rat visual cortex. I. The pyramidal cells. *J Comp Neurol* 234:218–241.
35. Sawtell NB, *et al.* (2003) NMDA receptor-dependent ocular dominance plasticity in adult visual cortex. *Neuron* 38:977–985.
36. Goel A, Lee HK (2007) Persistence of experience-induced homeostatic synaptic plasticity through adulthood in superficial layers of mouse visual cortex. *J Neurosci* 27:6692–6700.
37. Mahendran C, Berl S (1977) Isolation of troponin-like complex from bovine brain cortex. *Proc Natl Acad Sci USA* 74:2273–2277.
38. Garaschuk O, Griesbeck O, Konnerth A (2007) Troponin C-based biosensors: A new family of genetically encoded indicators for in vivo calcium imaging in the nervous system. *Cell Calcium* 42:351–361.
39. Heim N, *et al.* (2007) Improved calcium imaging in transgenic mice expressing a troponin C-based biosensor. *Nat Methods* 4:127–129.
40. Turrigiano GG, Nelson SB (2004) Homeostatic plasticity in the developing nervous system. *Nat Rev Neurosci* 5:97–107.
41. Desai NS, Cudmore RH, Nelson SB, Turrigiano GG (2002) Critical periods for experience-dependent synaptic scaling in visual cortex. *Nat Neurosci* 5:783–789.
42. Sara Y, *et al.* (2005) Selective capability of SynCAM and neuroligin for functional synapse assembly. *J Neurosci* 25:260–270.
43. Maffei A, Nelson SB, Turrigiano GG (2004) Selective reconfiguration of layer 4 visual cortical circuitry by visual deprivation. *Nat Neurosci* 7:1353–1359.
44. Mrsic-Flogel TD, *et al.* (2007) Homeostatic regulation of eye-specific responses in visual cortex during ocular dominance plasticity. *Neuron* 54:961–972.
45. Derkach VA, Oh MC, Guire ES, Soderling TR (2007) Regulatory mechanisms of AMPA receptors in synaptic plasticity. *Nat Rev Neurosci* 8:101–113.
46. Ishikawa R, Kohama K (2007) Actin-binding proteins in nerve cell growth cones. *J Pharmacol Sci* 105:6–11.
47. Harris KM (1999) Structure, development, and plasticity of dendritic spines. *Curr Opin Neurobiol* 9:343–348.
48. Oray S, Majewska A, Sur M (2004) Dendritic spine dynamics are regulated by monocular deprivation and extracellular matrix degradation. *Neuron* 44:1021–1030.
49. Kennedy MB, Beale HC, Carlisle HJ, Washburn LR (2005) Integration of biochemical signalling in spines. *Nat Rev Neurosci* 6:423–434.
50. Jiang WS, Yin ZQ (2007) Screening of genes associated with termination of the critical period of visual cortex plasticity in rats. *Curr Eye Res* 32:709–716.
51. Fields RD (2005) Myelination: An overlooked mechanism of synaptic plasticity? *Neuroscientist* 11:528–531.